Math. Model. Nat. Phenom. 16 (2021) 58
https://doi.org/10.1051/mmnp/2021050

Mathematical Modelling of Natural Phenomena
www.mmnp-journal.org

NONLINEAR STATE-DEPENDENT PULSE CONTROL FOR AN SIRS EPIDEMIC MODEL WITH VARYING SIZE AND ITS APPLICATION TO THE TRANSMISSION OF BRUCELLOSIS

Lin-Fei Nie*, Fuwei Zhang and Lin Hu

Abstract. As the disease spreads, it will inevitably cause important damage to the life and health of the population, resulting in changes in the population quantity. In addition, in some economically underdeveloped areas, limited medical resources will also have an important impact on the prevention and control of diseases. Based on these, a susceptible-infected-recovered-susceptible (SIRS) epidemic model is established, where state-dependent pulse control strategy, varying total population and limited medical resources are introduced. By using the qualitative theory of ordinary differential equation, differential inequality techniques, Poincaré map, and other methods, some sufficient conditions of the existence and orbital asymptotical stability of positive order-1 or order-2 periodic solution are obtained in various situations. Theoretical results imply that the proportion of infected class can be controlled at a desired low level for a long time and disease will not break out among population. Finally, based on realistic parameters of brucellosis in ruminants, numerical simulations have been performed to expalin/extend our analytical results and the feasibility of the state-dependent feedback control strategy.

Mathematics Subject Classification. 34A37, 34D23, 92D30.

Received October 15, 2020. Accepted October 16, 2021.

1. Introduction

Brucellosis is one of the world's major zoonoses disease, which is caused by different species of Brucella, and can be transmitted to other animals and humans with exposure to infected animals or their products. In animals, brucellosis mainly causes weight loss, abortion, and reduces survival of newborns [25]. According to a study published in 2002, an estimated 10–13% of farm animals are infected with Brucella species, and annual losses were calculated to be around 60 million dollars. For example, the bison population in Yellowstone National Park (YNP) has long been infected with Brucella abortus, the bacterium causing bovine brucellosis. As a portion of the Yellowstone bison population periodically moves between habitats in the park and adjacent lands in Montana during winter, resulting in a risk of brucellosis transmission from migratory bison to livestock on overlapping ranges adjacent to the park [7]. Bacteria also can spread to humans if people come in contact with infected meat or the placenta of infected animals, or if someone eats or drinks unpasteurized milk or cheese.

Keywords and phrases: SIRS model with varying size, nonlinear state-dependent vaccination, order-k periodic solution, orbital stability, brucellosis.

College of Mathematics and System Science, Xinjiang University, Urumqi 830017, P.R. China.

* Corresponding author: lfnie@163.com

In humans, mortality is negligible, but the illness can last for several years. For many years, brucellosis not only brings serious economic losses, but also represents a significant public health burden on governments.

To understand brucellosis transmission dynamics, several mathematical models have been proposed to manage the risk of brucellosis transmission. Particularly, Abatih *et al.* [1] proposed a mathematical model previously proposed for the transmission dynamics of brucellosis among bison, and discussed the existence and stability of steady-state solutions of this model. Aïnseba *et al.* [2] formulated a model for brucellosis including vertical transmission and direct and indirect contamination of individuals, and analyse the asymptotic behaviour of this model. Lolika *et al.* [17] introduced a non-autonomous dynamical system to consider the effects of seasonality on brucellosis infection. Other investigations can be found in [5, 6, 8, 32, 33] and the references therein, to just mention a few.

Since 1932, government agencies have undertaken efforts to contain the disease and several licensed live Brucella vaccines are available for use in livestock. Currently, all cattle of ages 3–8 months are required to be given the Brucella abortus strain 19 vaccine. Vaccination of uninfected animals and culling of the infected animals have been successfully used to eradicate Brucellosis from most of the USA [30]. From a mathematical modeling perspective, references [11, 16, 20] considered the influence of the effectiveness of the vaccination on brucellosis prevention and brucella spread. Particularly, Nannyonga *et al.* [19] expanded existing model of brucellosis virus with direct, indirect, and vertical transmission to a model with culling effects, and analysed the stability, sensitivity and optimal control of this model.

However, more work has been done on existing models with continuous vaccination strategy, that is, assuming the vaccination is done instantaneously regardless of the proportion of susceptible and infected individuals in the population and cost of management. In fact, in some underdeveloped areas, especially in areas with limited medical resources, control measures are usually implemented only when the proportion of infected class is relatively high, or the proportion of the susceptible classes reaches a critical level. This type of control measures depends on the state of infected subjects (or susceptible subjects) and is called a state-dependent pulse control strategy (SPCS). Obviously, the SPCS is more reasonable and suitable for disease control or population control. Recently, a few mathematical models concerning SPCS have been proposed and investigated due to its economic, high efficiency and feasibility. Particularly, Tang *et al.* [28] proposed an SIR epidemic model with SPCS to investigate the effects of implementing control strategy to evaluate the feasibility and expense of disease control over an extended period. Nie *et al.* [21] studies an SIRS epidemic model with state-dependent pulse vaccination and medication control strategy, and presented sufficient conditions on the existence and orbital stability of positive order-1 or order-2 periodic solution. This idea can also be found in many other areas with threshold control strategy, such as virus control models [22], pest management models [35], population models [27, 31], and neuron models [29].

Additionally, traditional brucellosis epidemic models did not consider the impact of limited medical resources on brucellosis transmission, which indicates that the medical resources such as drugs, vaccine, equipment, and costs are sufficient to control brucellosis. Actually, in reality, the control of diseases in wild life is very expensive and medical institutions have an appropriate or limited capacity for immunization and drug treatment. Consequently, study epidemic models with limited medical resources revisited not only have important theoretical significance, but also have extremely important practical significance. Based on these, Qin *et al.* [23] investigated the dynamics of an SIR epidemic with resource limitation, and discussed the effects of without resource limitation and with resources limitation on eradicate an infectious disease. An SIR epidemic model with limited medical resources and lifelong immunity was considered by Zhao *et al.* [34], in which the stability and global asymptotical stability of disease-free periodic solution are proven, and some sufficient conditions for the existence of positive periodic solution are obtained.

Another typical feature that can be considered as a shortcoming is that the majority of the studies in mathematical epidemiology are dealing with epidemic models where the total population size is fixed. Such an assumption is appropriate if the disease spreads rapidly in a short period of time (such as, influenza, SARS), and that diseases-related deaths are insignificant in terms of their effect on the whole population. However, it clearly fails to hold for diseases that are endemic in communities with changing populations, and for diseases (smallpox, malaria, HIV/AIDS) which raise the mortality rate substantially. In recent years, a number of epidemic models

with varying total population have been developed subsequently to establish effective prevention and control strategies [12, 14, 15, 18]. For instance, Busenberg *et al.* [4] considered the dynamics of a class of HIV virus model with varying total population. Authors obtained thresholds for the persistence of the disease, and the global behavior of the solutions is also studied. Of course, there is still a lot of research that has not been mentioned, and research on this topic continues all the time.

To better understand the effects of state-dependent pulse control, the limited medical resources and the effects of population change on the transmission of brucellosis between animals, we developed a model incorporating a state-dependent pulse control strategy in a general SIRS epidemic model with varying total population size. The rest of this paper is structured as follows. In the next Section, we describe our model and briefly introduce some definitions and fundamental results which will be essential for our future discussions. In Section 3, the dynamics of state-dependent control model is characterized by discussing the existence and stability of positive order-1 or order-2 periodic solution. The paper ends with some interesting biological significance and numerical simulations, which validate our theoretical findings and the feasibility of the state-dependent pulse control strategy.

2. Model formulation and preliminaries

Busenberg *et al.* [3] proposed the following SIRS epidemic model with varying total population size.

$$\begin{cases} \frac{\mathrm{d}S(t)}{\mathrm{d}t} = bN(t) - \mathrm{d}S(t) - \frac{\lambda S(t)I(t)}{N(t)} + eR(t), \\ \frac{\mathrm{d}I(t)}{\mathrm{d}t} = \frac{\lambda S(t)I(t)}{N(t)} - (d + c + \varepsilon)I(t), \\ \frac{\mathrm{d}R(t)}{\mathrm{d}t} = cI(t) - (d + e + \delta)R(t). \end{cases} \tag{2.1}$$

Here, $S(t)$, $I(t)$, and $R(t)$ represent the numbers of susceptible, infected and recovered population at time t, respectively, $N(t) = S(t) + I(t) + R(t)$ is the time varying total population size. It is assumed that all susceptible population becomes infected at a rate of $\frac{\lambda I(t)}{N(t)}$, where $\lambda > 0$ is the effective per capita contract rate of infected bison population. All parameter values are assumed to be nonnegative and b, $c > 0$. A more detailed description of model (2.1) can be found in reference [3].

Based on the characteristics of the spread of brucellosis, model (2.1) is appropriate for brucellosis transmission. In classical epidemic models, the vaccination rate of susceptible individuals is assumed to be proportional to the number of susceptible individuals. However, for brucellosis among bison, vaccination success rate could has some saturation phenomenon of the limited medical resources, which depends on the number of susceptible bison population at time t. In order to characterize the saturation phenomenon, we can define the vaccination rate $p(t)$ as follows $p(t) = \frac{p_{\max} S(t)}{(S(t)+\theta(t))}$, $0 \le p_{\max} < 1$. Here, $p_{\max}$ $(0 \le p_{\max} < 1)$ denotes the maximal vaccination proportion and $\theta(t)$ is the half-saturation coefficient, that is, the number of susceptible bison when the vaccination rate is half to the largest vaccination rate. Although this vaccination rate is more complex to deal with than the constant one, it seems more reasonable to better describe the medical resources limitation in reality of the situation [10, 23].

For model (2.1), which take into account the medical resources limitedness and state-dependent pulse vaccination, we further introduce the following assumption.

(A) When the proportion of the infected bison individuals in the population reaches a certain critical level H and the proportion of the susceptible bison individuals in the population satisfied $\frac{S(t)}{N(t)} > G(H)$ at time $t_i(H)$, vaccination strategy is taken, which leads to the number of susceptible and recovered bison individuals immediately become

$$\left[1 - \frac{p_{\max} S(t_i(H))}{S(t_i(H)) + \theta(t_i(H))}\right] S(t_i(H)), \quad R(t_i(H)) + \frac{p_{\max} S^2(t_i(H))}{S(t_i(H)) + \theta(t_i(H))},$$

TABLE 1. Parameter, definitions, values and source of model (2.2).

Param.	Definition	Value	Source
b	Birth rate of bison population (year^{-1})	$[0.012, 0.12]$	–
d	Disease free death rate constant of bison population (year^{-1})	$[0.04, 0.07]$	[1]
ε	Excess per capita death rate of infected bison population (year^{-1})	0.05	[1]
δ	Excess per capita death rate of recovered bison population (year^{-1})	$[0, 1]$	–
c	Recovery rate of the infected bison population (year^{-1})	0.5	[1]
e	Per capita loss of immunity rate for recovered bison population (year^{-1})	0.2	[1]
λ	Transmission coefficient between compartments S and I (year^{-1})	$[0.05, 10]$	[1]
$p_{\max}$	Maximal vaccination proportion for susceptible bison population	$[0, 1]$	–
α	Ratio of half saturation coefficient $\theta(t)$ and total population size $N(t)$	$[0, 1]$	–

respectively. Here, $G(H) = \frac{[(b+c+\varepsilon-\delta)+(\delta-\varepsilon)H]}{(\lambda-\delta)}$, which is a threshold value and determines by the intersection of equation $\frac{\mathrm{d}(I(t)/N(t))}{\mathrm{d}t} = 0$ and control line $\frac{I(t)}{N(t)} = H$.

Based on the above assumption, an SIRS epidemic model with control strategies reads as follows

$$\begin{cases} \left.\begin{aligned} \frac{\mathrm{d}S(t)}{\mathrm{d}t} &= bN(t) - \mathrm{d}S(t) - \frac{\lambda S(t)I(t)}{N(t)} + eR(t) \\ \frac{\mathrm{d}I(t)}{\mathrm{d}t} &= \frac{\lambda S(t)I(t)}{N(t)} - (d+c+\varepsilon)I(t) \\ \frac{\mathrm{d}R(t)}{\mathrm{d}t} &= cI(t) - (d+e+\delta)R(t) \end{aligned}\right\} \frac{I(t)}{N(t)} < H, \text{ or } \frac{I(t)}{N(t)} = H \\ \text{and } 0 < \frac{S(t)}{N(t)} < G(H), \\ \left.\begin{aligned} S(t^+) &= \left(1 - \frac{p_{\max}S(t)}{S(t)+\theta(t)}\right) S(t) \\ I(t^+) &= I(t) \\ R(t^+) &= R(t) + \frac{p_{\max}S^2(t)}{S(t)+\theta(t)} \end{aligned}\right\} \frac{I(t)}{N(t)} = H \text{ and } \frac{S(t)}{N(t)} > G(H), \end{cases} \tag{2.2}$$

where $S(t^+)$, $I(t^+)$, and $R(t^+)$ denotes the numbers of susceptible, infected, and vaccinated bison after a pulse vaccination applied at time t, respectively. The model parameters can be obtained from published reports and articles on bison in the YNP, and are presented in Table 1.

The total size of bison is $N(t) = S(t) + I(t) + R(t)$, which satisfies

$$\frac{\mathrm{d}N(t)}{\mathrm{d}t} = (b-d)N(t) - \varepsilon I(t) - \delta R(t).$$

Clearly, the total population size $N(t)$ cannot be maintained at a stationary state, except for some special cases. In that case, it is often necessary to consider the proportions of individuals in the three epidemiological classes rather than absolute numbers. To do this, we define the new variables

$$x(t) = \frac{S(t)}{N(t)}, \quad y(t) = \frac{I(t)}{N(t)}, \quad z(t) = \frac{R(t)}{N(t)}. \tag{2.3}$$

Using the transformation (2.3), model (2.2) can be written as

$$\left\{\begin{array}{ll}\left.\begin{array}{rl}\frac{\mathrm{d}x(t)}{\mathrm{d}t} = & b-bx(t)+ez(t)-(\lambda-\varepsilon)x(t)y(t)+\delta x(t)z(t)\\ \frac{\mathrm{d}y(t)}{\mathrm{d}t} = & \lambda x(t)y(t)+\varepsilon y^2(t)+\delta y(t)z(t)-(b+c+\varepsilon)y(t)\\ \frac{\mathrm{d}z(t)}{\mathrm{d}t} = & cy(t)+\varepsilon y(t)z(t)+\delta z^2(t)-(b+e+\delta)z(t)\end{array}\right\} & y(t)<H, \text{ or } y(t)=H\\ & \text{and } 0<x(t)<G(H),\\ \left.\begin{array}{rl}x(t^+) = & \left(1-\frac{p_{\max}x(t)}{x(t)+\alpha}\right)x(t)\\ y(t^+) = & y(t)\\ z(t^+) = & z(t)+\frac{p_{\max}x^2(t)}{x(t)+\alpha}\end{array}\right\} & y(t)=H \text{ and } x(t)>G(H).\end{array}\right. \tag{2.4}$$

Remark 2.1. Considering that the half-saturation coefficient $\theta(t)$ changes with the total number of populations $N(t)$, we might as well assume that $\frac{\theta(t)}{N(t)}$ is a constant here. That is, we may assume that $\frac{\theta(t)}{N(t)}=\alpha$ $(0<\alpha<1)$ holds for all $t\geq 0$, where, α represents the degree of restriction about medical resources.

Before investigating the dynamics of model (2.4), it is necessary to have a clear view of the dynamics of model (2.4) without pulse control strategy which is well studied and some intersecting results have been achieved in reference [3]. In it, authors defined three pertinent threshold parameters as follows

$$\mathcal{R}_0=\frac{\lambda}{(b+c+\varepsilon)},\ \mathcal{R}_1=\left\{\begin{array}{ll}\frac{b}{d}, & \mathcal{R}_0\leq 1,\\ \frac{b}{d+\varepsilon y_e+\delta z_e}, & \mathcal{R}_0>1,\end{array}\right.\ \mathcal{R}_2=\left\{\begin{array}{ll}\frac{\lambda}{c+d+\varepsilon}, & \mathcal{R}_0\leq 1,\\ \frac{\lambda x_e}{c+d+\varepsilon}, & \mathcal{R}_0>1,\end{array}\right.$$

where $x_e=1-y_e-z_e$, $y_e=((\delta-\lambda)z_e+\lambda-b-c-\varepsilon)/(\lambda-\varepsilon)$, and z_e can be found by solving equation

$$\lambda(\delta-\varepsilon)z_e^2+[-\lambda(b+c+e+\delta-\varepsilon)+\varepsilon(e-c+\delta-\varepsilon)+c\delta]z_e+c(\lambda-b-c-\varepsilon)=0. \tag{2.5}$$

On the biological explanation of the pertinent threshold parameters $\mathcal{R}_0$, $\mathcal{R}_1$ and $\mathcal{R}_2$ are discussed in detail on page 261 of reference [3]. And for equation (2.5), there exists a unique positive root for $\mathcal{R}_0>1$. On the existence and stability of model (2.4) without pulse control strategy, we summarize the following Lemma 2.2, which is the main content of Theorem 2.1 in reference [3].

Lemma 2.2. *For model (2.4) without pulse control strategy, the following results hold.*

(*i*) *If* $\mathcal{R}_0\leq 1$, $\mathcal{R}_1<1$ *and* $\mathcal{R}_2<1$, *then* $N(t)\to 0$, $(x,y,z)\to(1,0,0)$ *and* $(S,I,R)\to(0,0,0)$ *as* $t\to\infty$.
(*ii*) *If* $\mathcal{R}_0>1$, $\mathcal{R}_1<1$ *and* $\mathcal{R}_2<1$, *then* $N(t)\to 0$, $(x,y,z)\to(x_e,y_e,z_e)$ *and* $(S,I,R)\to(0,0,0)$ *as* $t\to\infty$.
(*iii*) *If* $\mathcal{R}_0\leq 1$, $\mathcal{R}_1>1$ *and* $\mathcal{R}_2<1$, *then* $N(t)\to\infty$, $(x,y,z)\to(1,0,0)$ *and* $(S,I,R)\to(\infty,0,0)$ *as* $t\to\infty$.
(*iv*) *If* $\mathcal{R}_0\leq 1$, $\mathcal{R}_1>1$ *and* $\mathcal{R}_2>1$, *then* $N(t)\to\infty$, $(x,y,z)\to(1,0,0)$ *and* $(S,I,R)\to(\infty,\infty,\infty)$ *as* $t\to\infty$.
(*v*) *If* $\mathcal{R}_0>1$, $\mathcal{R}_1>1$ *and* $\mathcal{R}_2>1$, *then* $N(t)\to\infty$, $(x,y,z)\to(x_e,y_e,z_e)$ *and* $(S,I,R)\to(\infty,\infty,\infty)$ *as* $t\to\infty$.

From the point of view of controlling the disease, we just consider the dynamics of model (2.4) with the case (*v*), that is, $\mathcal{R}_0>1$, $\mathcal{R}_1>1$ and $\mathcal{R}_2>1$.

Remark 2.3. In fact, from the conclusion (*iv*) of Lemma 2.2, it's not hard to find that although the $y(t)=I(t)/N(t)\to 0$, the disease is persistent ($I(t)\to\infty$) as $t\to\infty$. Obviously, our modeling idea is not suitable for this case. How to propose a reasonable state dependent control model for this case will be an interesting problem.

Noticing that $z(t) = 1 - x(t) - y(t)$, it suffices to consider the following equivalent model of (2.4)

$$\left\{\begin{array}{ll} \frac{\mathrm{d}x(t)}{\mathrm{d}t} = & b - bx(t) - (\lambda - \varepsilon)x(t)y(t) + (\delta x(t) + e)(1 - x(t) - y(t)) \\ \frac{\mathrm{d}y(t)}{\mathrm{d}t} = & \lambda x(t)y(t) + \varepsilon y^2(t) - (b + c + \varepsilon)y(t) + \delta y(t)(1 - x(t) - y(t)) \\ x(t^+) = & \left(1 - \frac{p_{\max} x(t)}{x(t)+\alpha}\right) x(t) \\ y(t^+) = & y(t) \end{array}\right. \begin{array}{l} \left.\begin{array}{l} \\ \\ \end{array}\right\} y(t) < H, \text{ or } y(t) = H \\ \text{and } 0 < x(t) < G(H), \\ \left.\begin{array}{l} \\ \\ \end{array}\right\} y(t) = H \text{ and } x(t) > G(H). \end{array} \tag{2.6}$$

From a biological viewpoint, we only focus on model (2.6) in the biological meaning region $\mathbb{D} = \{(x(t), y(t)) : x(t) \geq 0, y(t) \geq 0, x(t) + y(t) \leq 1\} \subset \mathbb{R}^2_+ := \{(x, y) : x \geq 0, y \geq 0\}$. In addition, the global existence and uniqueness properties of solution of model (2.6) are guaranteed by the smoothness of the first two equations of model (2.6). For more details see reference [13].

The following result is on the nonnegative of solutions for model (2.6).

Lemma 2.4. *Assume that $(x(t), y(t))$ is the solution of model (2.6) with the initial condition $(x(t_0), y(t_0)) \in \mathbb{D}$. Then $(x(t), y(t)) \in \mathbb{D}$ for all $t \geq t_0$.*

The proof of Lemma 2.4 is similar to Lemma 2.1 and Lemma 1 in references [21] and [10], respectively, hence we omit it here.

In order to study the dynamics of model (2.6), we could define two cross-section to (2.6) by

$$\Gamma_1 := \{(x(t), y(t)) : 0 < x(t) < G(H), y(t) = H\}, \quad \Gamma_2 := \{(x(t), y(t)) : x(t) > G(H), y(t) = H\}.$$

Choosing section Γ_1 as Poincaré section and suppose that for any point $P_n(x_n, H) \in \Gamma_2$, the trajectory $O^+(P_n, t_0)$ initiating from point P_n will jump to section Γ_1 at point $P_n^+(x_n^+, H)$ due to pulse effect. Here we assume that $p_1^* < p_{\max} < 1$, and

$$p_1^* = \frac{(1 - H - G(H))(1 - H + \alpha)}{(1 - H)^2}. \tag{2.7}$$

It means that for any solution that lie in section Γ_2 will jump to section Γ_1 after once pulse effect. Furthermore, the point P_n^+ will intersects section Γ_2 at point $P_{n+1}(x_{n+1}, H)$. Repeat above-mentioned process, we can get two pulse points sequences $\{P_n^+(x_n^+, H)\}$, $\{P_n(x_n, H)\}$ $(n = 1, 2, \cdots)$ and $x_n^+ = x_n - \frac{p_{\max} x_n^2}{(x_n+\alpha)}$, which is entirely determined by x_n, $p_{\max}$, α and H. Then for any $n \in \mathbb{N} = \{1, 2, \cdots\}$, the associated Poincaré map defined on section Γ_1 is given by $\mathcal{F} : \Gamma_1 \to \Gamma_1$, $(x_n^+, H) \mapsto (x_{n+1}^+, H)$. That is,

$$x_{n+1}^+ := \mathcal{F}(x_n^+, p_{\max}, \alpha, H), \quad p_1^* < p_{\max} < 1. \tag{2.8}$$

This can be proved that function $\mathcal{F}$ is continuously differential and monotonically decreasing on $[0, G(H))$.

Next, we consider the following generalized planar state-dependent pulse differential equations

$$\left\{\begin{array}{lll} \frac{\mathrm{d}u}{\mathrm{d}t} = f(u, v), & \frac{\mathrm{d}v}{\mathrm{d}t} = g(u, v), & \varphi(u, v) \neq 0, \\ \triangle u = \xi(u, v), & \triangle v = \eta(u, v), & \varphi(u, v) = 0, \end{array}\right. \tag{2.9}$$

where $(u, v) \in \mathbb{R}^2$, we denote $\Delta u = u(t^+) - u(t)$, and $\Delta v = v(t^+) - v(t)$. Functions $f(u, v)$, $g(u, v)$, $\xi(u, v)$, $\eta(u, v)$ are continuous differentiable functions defined on $\mathbb{R}^2 = \{(u, v) : u, v \in (-\infty, +\infty)\}$ and $\varphi(u, v)$ is a sufficiently smooth function with $\mathbf{grad}\varphi(u, v) \neq 0$.

Let $\mathbb{S} \subset \mathbb{R}^2$ be an arbitrary nonempty set and $P_0 \in \mathbb{R}^2$ be an arbitrary point. The distance between P_0 and $\mathbb{S}$ is defined by $\rho(P_0, \mathbb{S}) = \inf_{P \in \mathbb{S}} |P - P_0|$. Set $X(t) = (u(t), v(t))$ be the solution of model (2.9) starting from

the initial point $X_0 \in \mathbb{R}^2$ at $t = t_0$. We define the positive orbit as follows

$$O^+(X_0, t_0) = \{X(t) = (u(t), v(t)) : t \geq t_0, X(t_0) = X_0\}.$$

Definition 2.5 (Orbital stability [9]). Trajectory $O^+(X_0, t_0)$ is said to be orbital stable if for any given $\varepsilon > 0$, there exists a constant $\delta = \delta(\varepsilon) > 0$ such that for any other solution $X^*(t)$ of model (2.9), $\rho(X^*(t), O^+(z_0, t_0)) < \varepsilon$ for all $t > t_0$ when $\rho(X^*(t_0), O^+(X_0, t_0)) < \delta$.

Definition 2.6 (Orbital asymptotical stability [9]). Trajectory $O^+(X_0, t_0)$ is said to be orbital asymptotical stable if it is orbital stable, and there exists a constant $\eta > 0$ such that for any other solution $X^*(t)$ of model (2.9), $\lim_{t\to\infty} \rho(X^*(t), O^+(X_0, t_0)) = 0$ when $\rho(X^*(t_0), O^+(X_0, t_0)) < \eta$.

Definition 2.7 (Order-k periodic solution [13]). A trajectory $O^+(X_0, t_0)$ of model (2.9) is said to be order-k periodic if exists a positive integer $k \geq 1$ such that k is the smallest integer for $x_n^+ = x_{n+k}^+$.

The following Lemma 2.8 comes from the Corollary 2 of Theorem 1 of reference [26], which is useful for determining the stability of positive periodic solution of (2.9).

Lemma 2.8 (Analogue of Poincaré criterion [26]). *The order-k positive periodic solution* $(u(t), v(t)) = (\phi(t), \psi(t))$ *of model* (2.9) *is orbital asymptotical stable and enjoys the property of asymptotic phase, if the multiplier* μ *satisfies*

$$|\mu| = \left| \prod_{j=1}^{n} \Delta_j \exp\left\{ \int_0^T \left[\frac{\partial f(\phi(t), \psi(t))}{\partial x} + \frac{\partial g(\phi(t), \psi(t))}{\partial y} \right] \mathrm{d}t \right\} \right| < 1$$

where,

$$\Delta_j = \frac{\left(\frac{\partial \eta}{\partial y}\frac{\partial \varphi}{\partial x} - \frac{\partial \eta}{\partial x}\frac{\partial \varphi}{\partial y} + \frac{\partial \varphi}{\partial x} \right) f_+ + \left(\frac{\partial \xi}{\partial x}\frac{\partial \varphi}{\partial y} - \frac{\partial \xi}{\partial y}\frac{\partial \varphi}{\partial x} + \frac{\partial \varphi}{\partial y} \right) g_+}{\frac{\partial \varphi}{\partial x} f + \frac{\partial \varphi}{\partial y} g},$$

and f, g, $\frac{\partial \xi}{\partial x}$, $\frac{\partial \xi}{\partial y}$, $\frac{\partial \eta}{\partial x}$, $\frac{\partial \eta}{\partial y}$, $\frac{\partial \varphi}{\partial x}$, *and* $\frac{\partial \varphi}{\partial y}$ *have been calculated at the point* $(\phi(\tau_j), \psi(\tau_j))$, $f_+ = f(\psi(\tau_j^+), \psi(\tau_j^+))$, $g_+ = g(\phi(\tau_j^+), \psi(\tau_j^+))$, *and* τ_j $(j \in N)$ *is the time of the jth jump.*

3. Main results

In this section, we mainly focus on the existence and stability of positive order-k ($k \geq 1$) periodic solution of model (2.6) under certain additional assumptions. From the geometrical construction of phase space of model (2.6), the trajectory $O^+(M, t_0)$ from any initial point $M \in \Gamma_1$ intersects section Γ_2 infinite times with $H \leq y_e$. However, if $H > y_e$, the trajectory $O^+(M, t_0)$ from any initial point $M \in \Gamma_1$ may be free from pulse effects or tend to the endemic equilibrium $E_1^*(x_e, y_e)$ experiences finitely many pulse, which depend on the initial conditions. In what follows, we discuss the two distinct cases of $H \leq y_e$ and $H > y_e$, respectively.

- Case I: The case of $H \leq y_e$

Theorem 3.1. *For any* $p_1^* < p_{\max} < 1$, *then model* (2.6) *exists a positive order-*1 *periodic solution, where* p_1^* *is given by equation* (2.7).

Proof. For any $p_1^* < p_{\max} < 1$, we can choose small enough positive constants η such that $\eta < G(H) - \frac{p_{\max} G^2(H)}{(G(H)+\alpha)}$. The trajectory $O^+(Q_0^+, t_0)$ of model (2.6) begins from point $Q_0^+(\eta, H) \in \Gamma_1$ intersects section Γ_2 at point $Q_1(x_1, H)$. At point Q_1 the trajectory $O^+(Q_0^+, t_0)$ instantly jumps to point $Q_1^+(x_1^+, H)$ on section Γ_1 due to

pulse effect. We get point Q_1^+ is on the right of point Q_0^+ due to the fact that $\eta < x_1^+ < G(H)$. Thus, we have the following inequality holding

$$\mathcal{F}(\eta, p_{\max}, \alpha, H) - \eta = x_1^+ - \eta > 0. \tag{3.1}$$

Furthermore, for any $p_1^* < p_{\max} < 1$, we can choose small enough positive constants ε_1 and δ such that

$$\varepsilon_1 + \delta < \frac{p_{\max} G^2(H)}{G(H) + \lambda_1 + \alpha}.$$

Suppose that the trajectory $O^+(P_0^+, t_0)$ starting from the initial point $P_0^+(G(H) - \varepsilon_1, H)$, which insects section Γ_2 at point $P_1(G(H) + \lambda_1, H)$. According to the relation of λ_1 and δ, we consider the following two cases.

($\mathbf{A}_1$) $\lambda_1 \leq \delta$. Assume that the trajectory $O^+(P_0^+, t_0)$ jumps to point $P_1^+(G(H) - \varepsilon_2, H)$ on section Γ_1 due to pulse effect. Then one has

$$\begin{aligned} G(H) - \varepsilon_2 =& \left(1 - \frac{p_{\max}(G(H) + \lambda_1)}{G(H) + \lambda_1 + \alpha}\right)(G(H) + \lambda_1) \\ <& G(H) + \lambda_1 - \frac{p_{\max} G^2(H)}{G(H) + \lambda_1 + \alpha} \\ <& G(H) + \lambda_1 - (\varepsilon_1 + \delta) < G(H) - \varepsilon_1. \end{aligned}$$

It is easy to see that point P_1^+ is on the left of point P_0^+. Hence,

$$\mathcal{F}(G(H) - \varepsilon_1, p_{\max}, \alpha, H) - (G(H) - \varepsilon_1) = (G(H) - \varepsilon_2) - (G(H) - \varepsilon_1) < 0. \tag{3.2}$$

($\mathbf{A}_2$) $\lambda_1 > \delta$. For this case, we can choose positive constant $\varepsilon_1^* < \varepsilon_1$ such that

$$\varepsilon_1^* + \delta < \frac{p_{\max} G^2(H)}{G(H) + \lambda_1 + \alpha}.$$

Hence the trajectory $O^+(\widetilde{P}_0^+, t_0)$ initiating from point $\widetilde{P}_0^+(G(H) - \varepsilon_1^*, H)$, and reaches section Γ_2 at point $\widetilde{P}_1(G(H) + \delta, H)$ and then point $\widetilde{P}_1$ maps to $\widetilde{P}_1^+(G(H) - \varepsilon_2^*, H)$ after pulse effect. From the third equation of (2.6), it follows that

$$\begin{aligned} G(H) - \varepsilon_2^* =& \left(1 - \frac{p_{\max}(G(H) + \delta)}{G(H) + \delta + \alpha}\right)(G(H) + \delta) \\ <& G(H) + \delta - \frac{p_{\max} G^2(H)}{G(H) + \delta + \alpha} \\ <& G(H) + \delta - \frac{p_{\max} G^2(H)}{G(H) + \lambda_1 + \alpha} \\ <& G(H) + \delta - (\varepsilon_1^* + \delta) = G(H) - \varepsilon_1^*. \end{aligned}$$

Then we have $\widetilde{P}_1^+$ is on the left of point $\widetilde{P}_0^+$. Therefore, another inequality holds

$$\mathcal{F}(G(H) - \varepsilon_1^*, p_{\max}, \alpha, H) - (G(H) - \varepsilon_1^*) = (G(H) - \varepsilon_2^*) - (G(H) - \varepsilon_1^*) < 0. \tag{3.3}$$

It follows from (3.1)–(3.3) that there exists a fixed point for Poincaré map (2.8), which corresponds to the positive order-1 periodic solution of (2.6). This proof is complete. □

Suppose that $(x(t),y(t))=(\phi(t),\psi(t))$ is a positive order-1 periodic solution of model (2.6) with period T, directly applying Lemma 2.8 we can obtain the stability of the order-1 periodic solution of model (2.6).

Theorem 3.2. *Assume that the Floquet multiplier μ satisfies the following condition*

$$|\mu|=\Delta_1\exp\left\{\int_0^T[-2b-e-c-\varepsilon-(3\delta+\lambda-3\varepsilon)\psi(t)-(2-\lambda)\phi(t)+2\delta]\,\mathrm{d}t\right\}<1, \tag{3.4}$$

where

$$\Delta_1=\frac{(\varepsilon-\delta)H+\delta-(b+c+\varepsilon)+(\lambda-\delta)\left(\phi(T)-\frac{p_{\max}\phi^2(T)}{\phi(T)+\alpha}\right)}{\delta-b-c-\varepsilon+(\lambda-\delta)\phi(T)+(\varepsilon-\delta)H}\times\left[1-\frac{p_{\max}\phi(T)(\phi(T)+2\alpha)}{(\phi(T)+\alpha)^2}\right],$$

then $(x(t),y(t))=(\phi(t),\psi(t))$ is orbital asymptotical stable.

Proof. In what follows, we suppose this periodic solution $(\phi(t),\psi(t))$ with period T intersects sections Γ_1 and Γ_2 at points $E^+\big(\phi(T)-\frac{p_{\max}\phi^2(T)}{(\phi(T)+\alpha)},H\big)$ and $E(\phi(T),H)$, respectively. Then, we have $(\phi(T),\psi(T))=(\phi(T),H)$, $(\phi(T^+),\psi(T^+))=\big(\phi(T)-\frac{p_{\max}\phi^2(T)}{(\phi(T)+\alpha)},H\big)$. According to model (2.6) and (2.9), we denote

$$\begin{aligned}f(x,y)&=b-bx(t)+e(1-x(t)-y(t))-(\lambda-\varepsilon)x(t)y(t)+\delta x(t)(1-x(t)-y(t)),\\ g(x,y)&=-(b+c+\varepsilon)y(t)+\lambda x(t)y(t)+\varepsilon y^2(t)+\delta y(t)(1-x(t)-y(t)),\end{aligned}$$

$\xi(x,y)=-\frac{p_{\max}x^2(t)}{(x(t)+\alpha)}$, $\eta(x,y)=0$, $\varphi(x,y)=y(t)-H$. The direct calculation shows that

$$\begin{aligned}\frac{\partial f}{\partial x}&=-b-e-(\lambda-\varepsilon)y(t)+\delta(1-2x(t)-y(t)),\\ \frac{\partial g}{\partial y}&=-(b+c+\varepsilon)+\lambda x(t)+2\varepsilon y(t)+\delta(1-x(t)-2y(t)),\\ \frac{\partial\xi}{\partial x}&=-\frac{p_{\max}x(t)(x(t)+2\alpha)}{(x(t)+\alpha)^2},\qquad \frac{\partial\varphi}{\partial y}=1,\qquad \frac{\partial\eta}{\partial x}=\frac{\partial\eta}{\partial y}=\frac{\partial\xi}{\partial y}=\frac{\partial\varphi}{\partial x}=0,\end{aligned}$$

and

$$\begin{aligned}\Delta_1=&\frac{\left(\frac{\partial\eta}{\partial y}\frac{\partial\varphi}{\partial x}-\frac{\partial\eta}{\partial x}\frac{\partial\varphi}{\partial y}+\frac{\partial\varphi}{\partial x}\right)f_+ +\left(\frac{\partial\xi}{\partial x}\frac{\partial\varphi}{\partial y}-\frac{\partial\xi}{\partial y}\frac{\partial\varphi}{\partial x}+\frac{\partial\varphi}{\partial y}\right)g_+}{\frac{\partial\varphi}{\partial x}f+\frac{\partial\varphi}{\partial y}g}\\ =&\frac{\left(1-\frac{p_{\max}x(t)(x(t)+2k)}{(x(t)+k)^2}\right)g_+(\phi(T^+),\psi(T^+))}{g(\phi(T),\psi(T))}\\ =&\frac{(\varepsilon-\delta)H+\delta-(b+c+\varepsilon)+(\lambda-\delta)\left(\phi(T)-\frac{p_{\max}\phi^2(T)}{\phi(T)+\alpha}\right)}{\delta-b-c-\varepsilon+(\lambda-\delta)\phi(T)+(\varepsilon-\delta)H}\left[1-\frac{p_{\max}\phi(T)(\phi(T)+2\alpha)}{(\phi(T)+\alpha)^2}\right].\end{aligned}$$

Further, it is easy to verify

$$\tfrac{\partial f(\phi(t),\psi(t))}{\partial x}+\tfrac{\partial g(\phi(t),\psi(t))}{\partial y}=-2b-e-c-\varepsilon-(3\delta+\lambda-3\varepsilon)\psi(t)-(2-\lambda)\phi(t)+2\delta.$$

Based on the above discussion and Lemma 2.8, as a general result of stability of the positive order-1 periodic solution of model (2.6), we have that if (3.4) holds, then the positive order-1 periodic solution $(\phi(t), \psi(t))$ is orbital asymptotical stable. The proof is complete. □

Next, integrating the second equation of model (2.6) along the orbit $\widetilde{EE^+}$, yield

$$\begin{aligned} 0 = \int_H^H \frac{\mathrm{d}y}{y} &= \int_0^T [-(b+c+\varepsilon) + \lambda x(t) + \varepsilon y(t) + \delta(1 - x(t) - y(t))]\,\mathrm{d}t \\ &= \int_0^T [-(b+c+\varepsilon) + \lambda \phi(t) + \varepsilon \psi(t) + \delta(1 - \phi(t) - \psi(t))]\,\mathrm{d}t \\ &> \int_0^T [-(b+c+\varepsilon) + \lambda \phi(t) + \varepsilon \psi(t) + \delta(1 - \phi(t) - 2\psi(t))]\,\mathrm{d}t. \end{aligned}$$

Hence, we have the following corollary of Theorem 3.2.

Corollary 3.3. *Let $(x(t), y(t)) = (\phi(t), \psi(t))$ be a positive order-1 periodic solution of model (2.6) with period T. If*

$$|\mu| = \Delta_1 \exp\left\{\int_0^T [-b - e - (\lambda - 2\varepsilon + \delta)\psi(t) + \delta - 2\phi(t)]\,\mathrm{d}t\right\} < 1,$$

then $(\phi(t), \psi(t))$ is orbital asymptotical stable.

In the following, we will state and demonstrate another criterion on the existence and stability of positive order-k ($k = 1, 2$) periodic solution of model (2.6).

Theorem 3.4. *If $p_1^* < p_{\max} < 1$, then model (2.6) has a positive order-1 or order-2 periodic solution, which is orbital asymptotical stable. Moreover, model (2.6) does not have periodic solutions with the order greater than or equal to 3.*

Proof. If $H \le y_e$ and $p_1^* < p_{\max} < 1$, then any trajectory of model (2.6) that starts from section Γ_1 will meet section Γ_2 infinite times. Choose any two points $P_i^+(x_i^+, H)$ and $P_j^+(x_j^+, H)$, satisfy $0 < x_i^+ < x_j^+ < G(H)$, then the solution of model (2.6) starts from point P_i^+ and P_j^+ will meet section Γ_2 at points $P_{i+1}(x_{i+1}, H)$ and $P_{j+1}(x_{j+1}, H)$, respectively. Furthermore, points P_{i+1} and P_{j+1} jump to section Γ_1 at point P_{i+1}^+ and P_{j+1}^+, respectively. Since function $\mathcal{F}$ is monotonically decreasing on $[0, G(H))$, it means that $0 < \mathcal{F}(x_j^+) < \mathcal{F}(x_i^+) < G(H)$, namely

$$0 < x_{j+1}^+ < x_{i+1}^+ < G(H). \tag{3.5}$$

Therefore, if $x_0^+ = x_1^+$, then model (2.6) exhibits a positive order-1 periodic solution. If $x_0^+ \neq x_1^+$ and $x_0^+ = x_2^+$, then model (2.6) has a positive order-2 periodic solution.

Now, we consider the general case, that is, $x_0^+ \neq x_1^+ \neq x_2^+ \neq \cdots \neq x_{k-1}^+$ ($k > 2$).

If $x_1^+ < x_0^+$, from (3.5) we obtain that $x_2^+ > x_1^+$. Furthermore, $x_1^+ < x_2^+ < x_0^+$ or $x_1^+ < x_0^+ < x_2^+$. If $x_0^+ < x_1^+$, it follows that $x_1^+ > x_2^+$ by (3.5). Then we must have, $x_0^+ < x_2^+ < x_1^+$ or $x_2^+ < x_0^+ < x_1^+$. Hence, for the relation of x_0^+, x_1^+, and x_2^+ we have following four possibilities.

(**a**) If $x_1^+ < x_2^+ < x_0^+$, we get $x_2 > x_3 > x_1$ and further $x_0^+ > x_2^+ > x_3^+ > x_1^+$. By induction, we get

$$0 < x_1^+ < x_3^+ < \cdots < x_{2k+1}^+ < \cdots < x_{2k}^+ < \cdots < x_2^+ < x_0^+ < G(H). \tag{3.6}$$

Performing the similar discussion to (**a**), we yield the following cases.

(**b**) If $x_1^+ < x_0^+ < x_2^+$, it follows

$$0 < \cdots < x_{2k+1}^+ < \cdots < x_3^+ < x_1^+ < x_0^+ < x_2^+ < \cdots < x_{2k}^+ < \cdots < G(H). \tag{3.7}$$

(**c**) If $x_0^+ < x_2^+ < x_1^+$, this show that

$$0 < x_0^+ < x_2^+ < \cdots < x_{2k}^+ < \cdots < x_{2k+1}^+ < \cdots < x_3^+ < x_1^+ < G(H). \tag{3.8}$$

(**d**) If $x_2^+ < x_0^+ < x_1^+$, it can be easily obtained that

$$0 < \cdots < x_{2k}^+ < \cdots < x_2^+ < x_0^+ < x_1^+ < x_3^+ < \cdots < x_{2k+1}^+ < \cdots < G(H). \tag{3.9}$$

If there exists a positive order-k ($k \geq 3$) periodic solution of model (2.6), then $x_{j-1}^+ \neq x_j^+$ ($j = 1, 2, \cdots, k-1$), $x_0^+ \neq x_{k-1}^+$ and $x_0^+ = x_k^+$, which is contradict to (3.6)–(3.9). Hence, we conclude that model (2.6) does not exhibit an order-k ($k \geq 3$) positive periodic solution.

From cases (**b**) and (**d**), it is easy to see that there are two different limits x_1^* and x_2^* with sequences $\{x_{2k}^+\}$ and $\{x_{2k+1}^+\}$ tending to x_1^* and x_2^*, respectively. From Poincaré map (2.8) we obtain, $x_1^* = \mathcal{F}(x_2^*, p_{\max}, k, H)$, $x_2^* = \mathcal{F}(x_1^*, p_{\max}, k, H)$. These conclusions imply that there is a positive order-2 periodic solution of model (2.6) which is orbital asymptotical stable. Similarly, for cases (**a**) and (**c**), it follows that model (2.6) has an orbital asymptotical stable positive order-1 periodic solution. The proof is complete. □

- Case II: The case of $H > y_e$

Theorem 3.5. *For the case $H > y_e$, one of the following statements holds.*

(*i*) *If there is a point $A \in \Gamma_1$, such that the trajectory $O^+(A, t_0)$ of model (2.6) from the initial point $A(x_A, H)$ is tangent to the line $y = H$ at point $B(G(H), H)$ and $p_2^* < p_{\max} < 1$, where*

$$p_2^* = \frac{(1 - H - x_A)(1 - H + \alpha)}{(1 - H)^2}, \tag{3.10}$$

then model (2.6) possesses an orbital asymptotical stable positive order-1 or order-2 periodic solution. Moreover, if $0 < p_{\max} < p_3^*$, where

$$p_3^* = \frac{(G(H) - x_A)(G(H) + \alpha)}{G^2(H)}, \tag{3.11}$$

then model (2.6) does not exhibit positive order-k ($k \geq 1$) periodic solution.

(*ii*) *If for any point $A \in \Gamma_1$, the trajectory $O^+(A, t_0)$ of model (2.6) from the initial point A intersects with section Γ_2 infinite times, then model (2.6) has a positive order-1 or order-2 periodic solution, which is orbital asymptotical stable. Moreover, model (2.6) does not exhibit positive order-k ($k \geq 3$) periodic solution.*

(*iii*) *If for any point $A \in \Gamma_1$, the trajectory $O^+(A, t_0)$ of model (2.6) from the initial point A does not intersects with section Γ_2, then model (2.6) has no positive order-k ($k \geq 1$) periodic solution.*

Proof. Firstly, we demonstrate (i). In view of the phase portrait of model (2.6), there is a point $A \in \Gamma_1$, such that the trajectory $O^+(A, t_0)$ of model (2.6) from initial point $A(x_A, H)$ is tangent to the line $y = H$ at point $B(G(H), H)$. Obviously, the trajectory of model (2.6) which starts from right of point A will not meet section Γ_2 and tend to the epidemic equilibrium $E_1^*(x_e, y_e)$. Therefore, we only need to consider the trajectory $O^+(A_1, t_0)$ of model (2.6) starting from initial point $A_1(x_{A_1}, H)$ ($0 < x_{A_1} < x_A$). If condition $p_2^* < p_{\max} < 1$ holds, it easy to see that any solution lies in section Γ_2 will jump to left of point A. Therefore, the trajectory $O^+(A_1, t_0)$ will

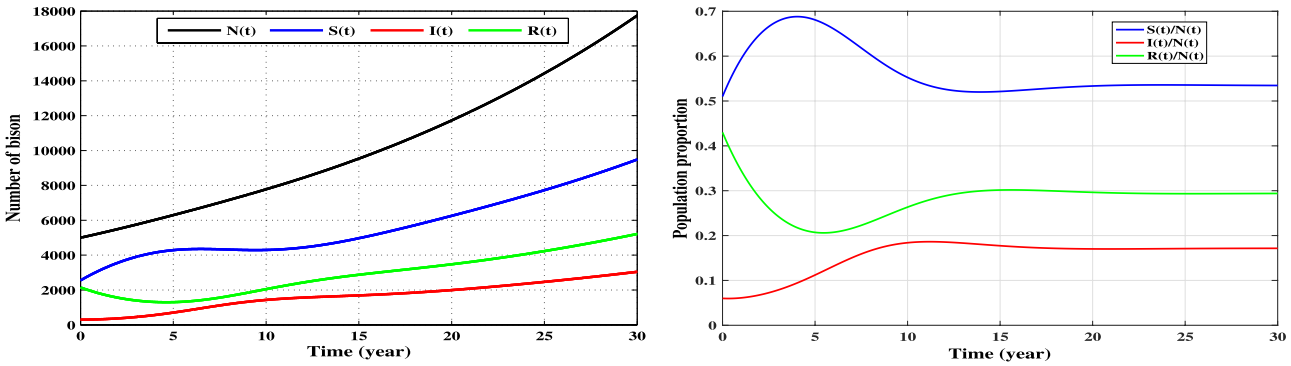

(a) (b)

FIGURE 1. Asymptotic behavior of model (2.1) and its transformed proportionate system for the case $\mathcal{R}_0 > 1$, $\mathcal{R}_1 > 1$, and $\mathcal{R}_2 > 1$: (a) Time series of $N(t)$, $S(t)$, $I(t)$, and $R(t)$; (b) Time series $S(t)/N(t)$, $I(t)/N(t)$, R(t)/N(t).

intersect section Γ_2 infinite times with $H > y_e$. Performing a similar process to Theorem 3.4, it yields model (2.6) has an orbital asymptotical stable positive order-1 or order-2 periodic solution. If $0 < p_{\max} < p_3^*$, which implies that any solution lies in section Γ_2 will jump to right of point A, and then tends to the epidemic equilibrium $E_1^*(x_e, y_e)$. Hence, model (2.6) does not exhibit positive order-k ($k \geq 1$) periodic solution for $H > y_e$.

Now we turn to (ii). If for any point $A \in \Gamma_1$, the trajectory $O^+(A, t_0)$ of model (2.6) from the initial point A intersects with section Γ_2 infinite times. Similar to (i), we can also obtain that model (2.6) possesses an orbital asymptotical stable positive order-1 or order-2 periodic solution with $H > y_e$.

Finally, we prove (iii). If for any point $A \in \Gamma_1$, the trajectory $O^+(A, t_0)$ of model (2.6) from the initial point A does not intersects with section Γ_2. It means that the trajectory $O^+(A, t_0)$ of model (2.6) directly tends to the epidemic equilibrium $E_1^*(x_e, y_e)$ due to epidemic equilibrium $E_1^*(x_e, y_e)$ being global asymptotical stable. Obviously, in this case, model (2.6) no exhibit positive order-k ($k \geq 1$) periodic solution with $H > y_e$. The proof is complete. □

Remark 3.6. From conclusion of part (i) of Theorem 3.5, we note that $p_{\max} \in (p_2^*, 1)$ is a sufficient condition for model (2.6) to have a positive order-1 or order-2 periodic solution. Meanwhile $p_{\max} \in (0, p_3^*)$ is also a sufficient condition for model (2.6) to have no positive periodic solution. However, for the case where $p_{\max} \in (p_3^*, p_2^*)$, the dynamics of model (2.6) will be very complex.

4. Numerical simulations and biological interpretations

In this section, based on the reported Yellowstone bison brucellosis data, some numerical investigations are performed to validate the feasibility of state-dependent control strategy on the transmission of brucellosis among bison. To this end, we set $b = 0.1$, $c = 0.5$, $\varepsilon = 0.05$, $\lambda = 1.2$, $d = 0.05$, $e = 0.2$, and $\delta = 0.0001$ by Table 1. Throughout this section, we shall assume that the unit of time is one year. Firstly, by directly calculating, we have $\mathcal{R}_0 = 1.8462 > 1$, $\mathcal{R}_1 = 1.7065 > 1$, and $\mathcal{R}_2 = 2 > 1$. Theoretical results and numerical simulations show that the numbers of susceptible $S(t)$, infected $I(t)$, recovered $R(t)$ and the total number of population $N(t)$ increase with time, but the proportions of susceptible, infected and recovered in the population remain constant as $t \to \infty$. That is, model (2.1) has a unique global asymptotical stable equilibrium $(x_e, y_e, z_e) = (S/N, I/N, R/N) = (0.5347, 0.1715, 0.2938)$. These are exactly what are shown in Figure 1a and 1b.

Further, we choose the control parameters to be $p_{\max} = 0.6$, $\alpha = 0.2$, $H = 0.06 < 0.1715 = y_e$, then we get

$$G(H) = \frac{[(b + c + \varepsilon - \delta) + (\delta - \varepsilon)H]}{(\lambda - \delta)} = 0.5391.$$

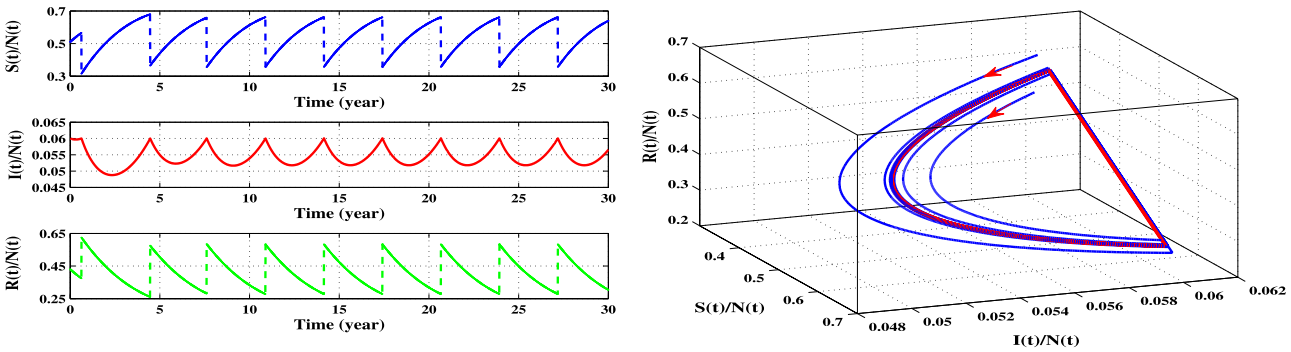

(a) (b)

FIGURE 2. The existence and stability of order-1 periodic solution of model (2.4): (a) the existence; (b) the orbital stability.

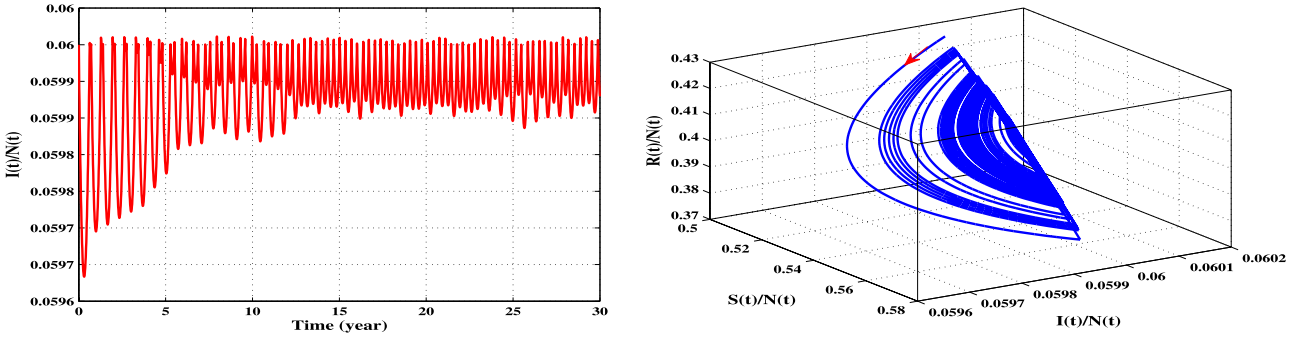

(a) (b)

FIGURE 3. The impact of threshold value p_1^* on disease control and elimination, where $H = 0.06 < 0.1715 = y_e$ and $p_{\max} = 0.06 < p_1^*$: (a) time series of $I(t)/N(t)$; (b) phase portrait.

It follows from equation (2.7) that we get $p_1^* = 0.4356 < p_{\max} = 0.6$. By Theorem 3.1, we know that model (2.2) exists a positive order-1 periodic solution which is shown in Figure 2a. Moreover, the stability of positive order-1 periodic solution is shown in Figure 2b. The existence of a global stable positive order-1 periodic solution means that if there are not enough medical resources (*e.g.*, vaccine, drugs, etc.) to eliminate brucellosis, state-dependent immunization is an effective way to both control brucellosis and keep the proportion of infected individuals at a desired low level for a long time.

Nextly, we consider the impact of threshold value p_1^* on disease control and elimination. The plots in Figure 3 show that the proportion of susceptible, infected, and recovered bison populations oscillate periodically with different periods and amplitudes. Numerical simulations imply that if the maximal vaccination proportion $p_{\max}$ is less than the threshold value p_1^*, for example, $p_{\max} = 0.074 < p_1^* = 0.4356$, frequent immunization will inevitably occur. This can lead to unnecessary waste of human and financial resources. Therefore, the greater immune rate $p_{\max}$ is essential to control the spread of the brucella virus, regardless of the lack of medical resources. In addition, Figure 4a–d respectively indicate the existence and orbital asymptotical stability of the order-2 periodic solution of model (2.6). Numerical simulation and theoretical results show that the introduction of nonlinear state dependent pulse control makes the dynamic behavior of the model more complex.

Additionally, it is as mentioned earlier that the strength of vaccination is the key factor to prevention and control the spread of diseases. To study this issue, we let the values of H and k be as mentioned before and choose $p_{\max}$ to be 0.6, 0.65, and 0.7, respectively. The plots in Figure 5a show that the proportion of the infected

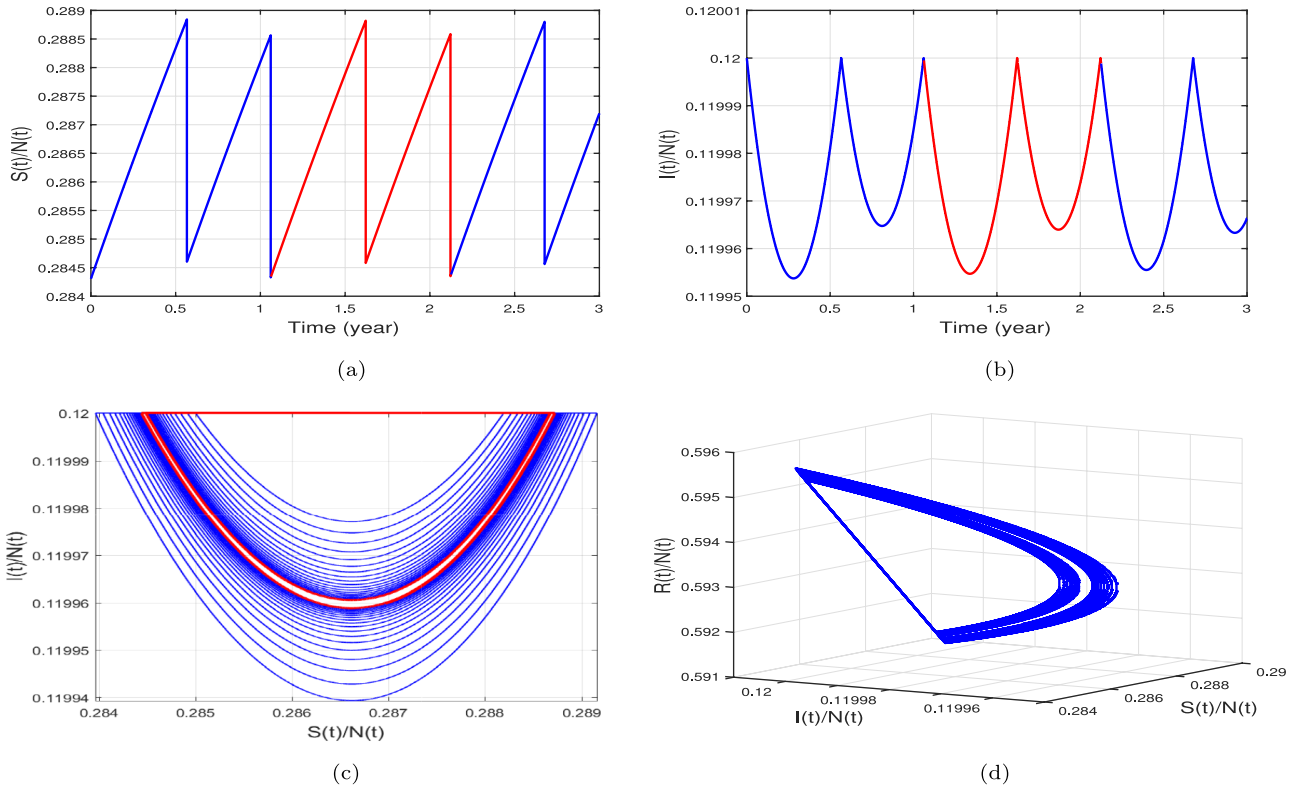

FIGURE 4. The existence and stability of order-2 periodic solution of model (2.6).

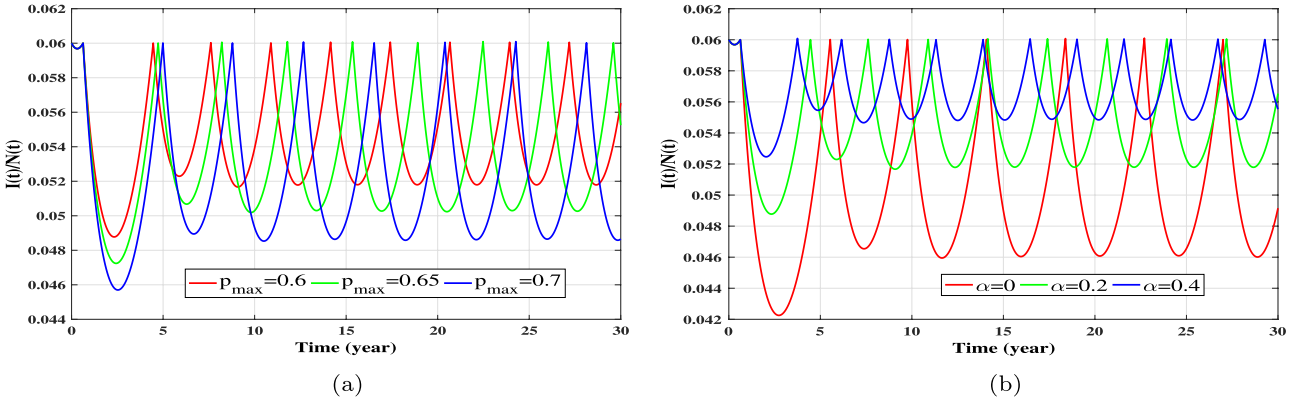

FIGURE 5. The effects of maximal pulse vaccination proportion $p_{\max}$ and resources limitation parameter α on the period and amplitude of positive order-1 periodic solution.

bison can be controlled within a lower range and the period of positive order-1 periodic solution of model (2.6) become longer with the increases of immune strength $p_{\max}$. It may be that, with limited medical resources, low frequency high immunization rate is more beneficial to control the spread of brucellosis than high frequency low immunization rate. Further, in order to address how resources limitation affect the dynamics of model (2.6), we let $p_{\max} = 0.6$ and $H = 0.06$ as mentioned before and α to be 0, 0.2, and 0.4, respectively. We note that if $\alpha = 0$, this is the case for without resources limitation, the proportion of the infected bison can be controlled

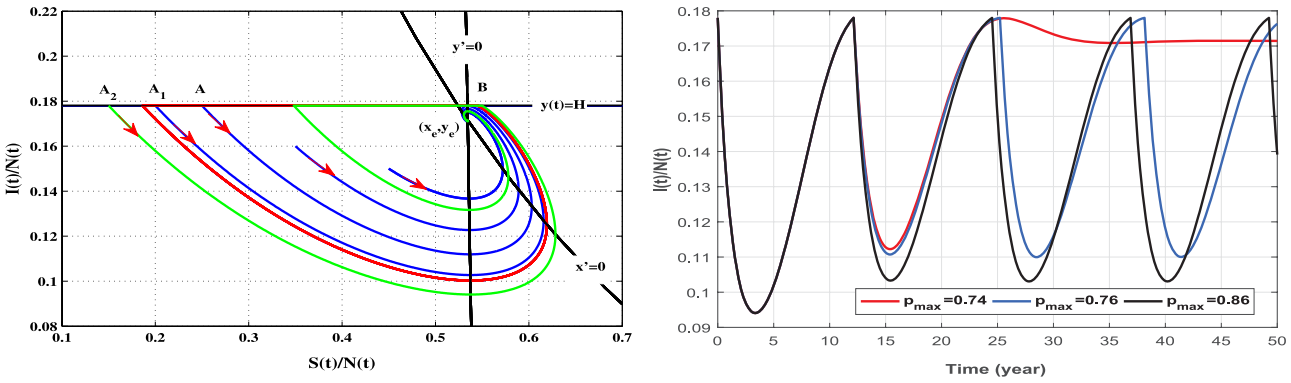

(a) (b)

FIGURE 6. The dynamics of model (2.6) with $H > y_e$: (a) the complex behaviors; (b) The effect of maximal vaccination proportion $p_{\max}$ for the dynamics of model (2.6).

within a certain range. However, if there is resources limitation, that is, the parameter α is larger than zero, then the periodic of positive order-1 periodic solution of model (2.6) decrease with the increases of parameter α, which are shown in Figure 5b. This theoretical results indicates that if we aim to keep the proportion of infected bison population at a desired low level, then it is necessary to carry out pulse vaccination more frequently under resources limitation than when medical resources are sufficient.

Finally, we will try to explain the dynamics of model (2.6) with $H > y_e$. It is easy to calculate that $p_2^* = 0.87$ and $p_3^* = 0.73$ by (3.10) and (3.11), respectively. Numerical simulation shows that (2.6) there exists a trajectory $O^+(A, t_0)$ starting from the initial point $A(x_A, H) = (0.25, 0.178)$ is tangent to the control line $y(t) = H$ at point $B(G(H), H) = (0.5342, 0.178)$. From the geometrical construction of phase space of model (2.6), we know that the trajectory of model (2.6) which starts from the right of point A will be free from pulse effects, and then tends to the epidemic equilibrium $E_1^*(x_e, y_e)$, which means that disease will continue persisting for a long time. However, the trajectory $O^+(A_1, t_0)$ of model (2.6) initiating from the left of point A will intersect section Γ_2 infinitely many times and there exists a positive order-1 periodic solution under condition $p_{\max} \in (p_2^*, 1)$, which is illustrated as in Figure 6a by the red line. That's what the first part of conclusion (i) in Theorem 3.5 is all about. However, if we choose $p_{\max} = 0.5 \in (0, p_3^*)$, numerical simulation shows that the trajectory $O^+(A_2, t_0)$ of model (2.6) initiating from left of point A intersect the section Γ_2 at most finitely many times and tend to the epidemic equilibrium $E_1^*(x_e, y_e)$, which is shown in Figure 6b by the green line. This is exactly what the second part of conclusion (i) in Theorem 3.5 says. The plots in Figure 6b explain the relations of the existence and stability of order-1 periodic solution with parameters $p_{\max}$, where $\alpha = 0.2$ and $p_{\max} = 0.74$, 0.76 and 0.86, respectively. As $p_{\max}$ decreases, the positive order-1 periodic solution loses its stability and the solutions of model (2.6) tend to the epidemic equilibrium $E_1^*(x_e, y_e)$. Therefore, for $H > y_e$, it is essential to select the appropriate immunization rate $p_{\max}$. At the same time, it is worth noticing that threshold value H less than y_e is an easier and more appropriate choice in real control of infectious disease. Of course, the community has the risk of the outbreak of disease for a large threshold value. Therefore, with the help of mathematical modeling, the optimal vaccination strategies can be properly designed.

Acknowledgements. We are grateful to the editors and the anonymous referees for their careful reading and helpful comments which led to great improvement of our paper. This research is partially supported by the Natural Science Foundation of Xinjiang Uygur Autonomous Region (Grant Nos. 2021D01E12 and 2021D01C070), the National Natural Science Foundation of China (Grant No. 11961066).

References

[1] E. Abatih, L. Ron, N. Speybroeck, B. Williams and D. Berkvens, Mathematical analysis of the tranmission dynamics of brucellosis among bison. *Math. Method. Appl. Sci.* **38** (2015) 3818–3832.

[2] B.E. Aïnseba, C. Benosman and P. Megal, A model for ovine brucellosis incorporating direct and indirect transmission. *J. Biol. Dyn.* **4** (2010) 2–11.

[3] S. Busenberg and P. van den Driessche, Analysis of a disease transmission model in a population with varying size. *J. Math. Biol.* **28** (1990) 257–270.

[4] S. Busenberg, K. Cooke and H. Thieme, Demographic change and persisitence of HIV/AIDS in a heterogengeous population. *SIAM J. Appl. Math.* **51** (1991) 1030–1052.

[5] R.S. Cantrell, C. Cosner and W.F. Faganantrell, Brucellosis, botflies, and brainworms: the impact of edge habitats on pathogen transmission and species extinction. *J. Math. Biol.* **42** (2001) 95–119.

[6] A. Dobson and M. Meagher, The population dynamics of Brucellosis in the Yellowstone national park. *Ecology* **77** (1996) 1026–1036.

[7] C. Geremia, P.J. White, J.A. Hoeting, R.L. Wallen, F.G.R. Watson, D. Blanton and N.T. Hobbs, Integrating population-and individual-level information in a movement model of Yellowstone bison. *Ecol. Appl.* **24** (2014) 346–362.

[8] J. González-Gunmán and R. Naulin, Analysis of a model of bovine brucellosis using singular perturbations. *J. Math. Biol.* **33** (1994) 211–223.

[9] J.K. Hale and H. Kocak, Dynamics and Bifurcations. Texts in Applied Mathematics, Springer-Verlag, New York (1991).

[10] Z.L. He, J.G. Li, L.F. Nie and Z. Zhao, Nonlinear state-dependent feedback control strategy in the SIR epidemic model with resource limitation. *Adv. Differ. Equ.-Ny* **2017** (2017) Article ID 209.

[11] Q. Hou, X. Sun, J. Zhang, Y. Liu, Y. Wang and Z. Jin, Modeling the transmission dynamics of sheep brucellosis in Inner Mongolia Autonomous Region, China. *Math. Biosci.* **242** (2013) 51–58.

[12] T. Kuniya and Y. Muroya, Global stability of a multi-group SIS epidemic model with varying total population size. *Appl. Math. Comput.* **265** (2015) 785–798.

[13] V. Lakshmikantham, D.D. Bainov and P.S. Simeonov, Theory of Impulsive Differential Equations. World Scientific, Singapore (1989).

[14] H. Li, R. Peng and F.B. Wang, Varying total population enhances disease persistence: Qualitative analysis on a diffusive SIS epidemic model. *J. Differ. Equ.* **262** (2017) 885–913.

[15] M.Y. Li, J.R. Graef, L. Wang and J. Karsai, Global dynamics of a SEIR model with varying total population size. *Math. Biosci.* **160** (1999) 191–213.

[16] M.T. Li, G.Q. Sun, Y.F. Wu, J. Zhang and Z. Jin, Transmission dynamics of a multi-group brucellosis model with mixed cross infection in public farm. *Appl. Math. Comput.* **237** (2014) 582–594.

[17] P.O. Lolika, S. Mushayabasa, C.P. Bhunu, C. Modnak and J. Wang, Modeling and analyzing the effects of seasonality on brucellosis infection. *Chaos Soliton. Fract.* **104** (2017) 338–349.

[18] G. Lu and Z. Lu, Global asymptotic stability for the SEIRS models with varying total population size. *Math. Biosci.* **296** (2018) 17–25.

[19] B. Nannyonga, G.G. Mwanga and L.S. Luboobi, An optimal control problem for ovine brucellosis with culling. *J. Biol. Dyn.* **9** (2015) 198–214.

[20] J. Nie, G.Q. Sun, X.D. Sun, J. Zhang, N. Wang, Y.M. Wang, C.J. Shen, B.X. Huang and Z. Jin, Modeling the transmission dynamics of dairy cattle brucellosis in Jilin province, China. *J. Biol. Syst.* **22** (2014) 533–554.

[21] L.F. Nie, Z.D. Teng and B.Z. Guo, A state dependent pulse control strategy for a SIRS epidemic system. *B. Math. Biol.* **75** (2013) 1697–1715.

[22] L.F. Nie, Z.D. Teng and I.H. Jung, Complex dynamic behavior in a viral model with state feedback control strategies. *Nonlinear Dyn.* **77** (2014) 1223–1236.

[23] W. Qin, S. Tang and R.A. Cheke, Nonlinear pulse vaccination in an SIR epidemic model with resource limitation. *Abstr. Appl. Anal.* **2013** (2013) 4339–4344.

[24] L.E. Samartino, Brucellosis in Argentina. *Vet. Microbiol.* **90** (2002) 71–80.

[25] M.M.H. Sewell and D.W. Brocklesby, Handbook of Animal Diseases in the Tropics, 4th edn. Balliere Tindall, Toronto (1990).

[26] P.S. Simeonov and D.D. Bainov, Orbital stability of periodic solutions of autonomous systems with impulse effect. *Int. J. Systems Sci.* **19** (1988) 2561–2585.

[27] S. Sun, C. Guo and C. Qin, Dynamic behaviors of a modified predator-prey model with state-dependent impulsive effects. *Adv. Differ. Equ.-Ny* **2016** (2016) Article ID 50.

[28] S. Tang, Y. Xiao and D. Clancy, New modelling approach concerning integrated disease control and cost-effectivity. *Nonlinear Anal.-Theory Methods Appl.* **63** (2005) 439–471.

[29] J. Touboul and R. Brette, Spiking dynamics of bidimensional integrate-and-fire neurons. *SIAM J. Appl. Dyn. Syst.* **8** (2009) 1462–1506.

[30] J.J. Treanor, J.S. Johnson, R.L. Wallen, S.Cilles, P.H. Crowley, J.J. Cox, D.S. Maehr, P.J. White and G.E. Plumb, Vaccination strategies for managing brucellosis in Yellowstone bison. *Vaccine* **28** (2010) F64–F72.

[31] Q. Xiao, B. Dai, B. Xu and L. Bao, Homoclinic bifurcation for a general state-dependent Kolmogorov type predator-prey model with harvesting. *Nonlinear Anal.-Real World Appl.* **26** (2015) 263–273.

[32] F. Xie and R.D. Horan, Disease and behavioral dynamics for brucellosis control in EIk and Cattle in the greater Yellowstone area. *J. Agric. Resour. Econ.* **34** (2009) 11–33.

[33] C. Yang, P.O. Lolika, S. Mushayabasa and J. Wang, Modeling the spatiotemporal variations in brucellosis transmission. *Nonlinear Anal.-Real World Appl.* **38** (2017) 49–67.
[34] W. Zhao, J. Li and X. Meng, Dynamical analysis of SIR epidemic model with nonlinear pulse vaccination and lifelong immunity. *Discrete Dyn. Nat. Soc.* **2015** (2015) Article ID 848623.
[35] T. Zhang, J. Zhang, X. Meng and T. Zhang, Geometric analysis of a pest management model with Holling's type III functional response and nonlinear state feedback control. *Nonlinear Dyn.* **84** (2016) 1529–1539.